International Journal of Academic Scientific Research
ISSN: 2272-6446 Volume 8, Issue 4 (November - December2020), PP 39-48
www.ijasrjournal.org

Modeling The Effect of Rotation and Traverse Speeds on Full Friction Stir Welding Process Using Coupled Eulerian- Lagrangian Analysis

Abdul Mounem Jesri[1], M. Jameel Alshehne[2], Shereen Hesso[3]

1 Department of Production Engineering, University of Aleppo, Syria
2 Department of Materials Engineering, University of Aleppo, Syria
3 Department of Production Engineering, University of Aleppo, Syria

ABSTRACT: *The Friction stir welding (FSW) process is a complex bonding technique which includes many of the associated physical phenomena. This paper presents a non-linear, three-dimensional, coupled thermo- mechanical model that simulates the full phases of the welding process (plunge, dwell and traverse) considering that the internal thermal source result of thermo-mechanical coupling and interaction of the interface, depending on a CEL analysis that combines the features of Eulerian and Lagrangian analysis using the Abaqus/Explicit program. The model was used to clarify effect of changing both of the rotational speed (315,630,1000) rpm and the traverse speed (60,150) mm/min in the maximum temperature and its distribution in addition to the stresses, applied to 6061-T6 aluminum alloy. The results of this study showed that numerical model with using CEL analysis allowed the modeling of large deformations that occur during FSW for the full phases, and also highlighted the main role of the rotation and traverse speeds in determining the maximum temperature and its distribution. As a result, the model showed that the welding process with a rotation speed of 315rpm and a traverse speed of 60 mm/min is the most appropriate, where the maximum temperature reached (70-90)% of the melting temperature of alloy 6061-T6 and is the thermal range for a successful FSW process. The numerical model was verified which corresponds to the results of experimental test which was done using a vertical milling machine that simulates a FSW machine.*

Keywords - *Friction Stir Welding: FSW, 6061-T6, Coupled Eulerian-Lagrangian: CEL*

I. INTRODUCTION

FSW method is a complex solid state joining process developed by TWI [1], able to weld metals with low melting point that are difficult to weld by conventional methods, especially aluminum alloys [2].

The general principle of FSW process is based on the use of a non-consumable rotating tool consisting of the probe and the shoulder of the tool. The probe is inserted into the edges of connecting the two plates until the shoulder comes into contact with the upper surface of the plates to be welded (the plunge phase), the rotating tool remains in place until the material becomes soft due to the heat generated from the plastic deformation and Frictional heating (the dwell phase) which leads to the material flow from the advance side to the retracting side. Then the tool moves along the edges of the two plates to accomplish the joint (the welding or traverse phase). Figure 1 illustrates the principle of FSW welding process [3].

Weld joint quality depend on FSW process parameters such as tool geometry, plunge depth, axial force, probe diameter and height, shoulder diameter, rotation and traverse speeds of the tool [4].

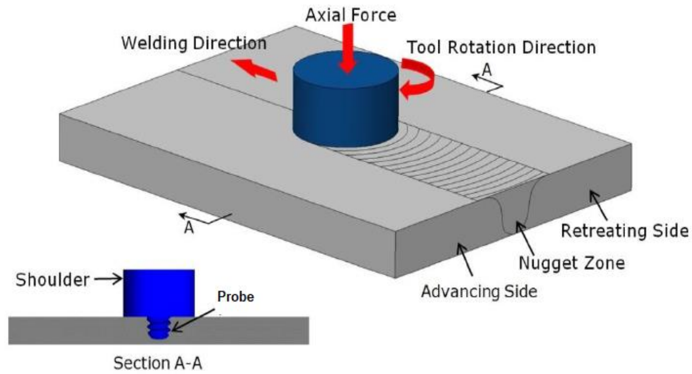

Figure. 1. Schematic drawing of FSW [3]

To study the effect of the process parameters, numerical modeling is often adopted using computational programs which are useful in understanding and visualizing the effect of these parameters on the FSW process in order to adjust and determine their values for obtain the best welding properties. The main criterion used to assess the success of the welding process is to reach the welding temperature to the range (70-90)% of the melting temperature of the welded plates. Here the modeling process allows for the determination of the temperature range and its distribution instead of experiments that consume time, cost and difficulty in using thermocouples in the nugget zone [1,5].

On the other hand, the numerical modeling of the FSW process faces many challenges due to the complications in the nature of the FSW process, which summoned most of the researchers to develop greatly simplified incomplete models that don't simulate the real process principle.

Muhsin et al.,[6] have used thermal numerical simulations to study rotational and traverse speeds of AA 7020-T53. Hongjun Li and Di Liu [7] have presented a simplified thermo-mechanical model with incomplete coupling using ANSYS software on AA6061-T6 in which the heat source was considered externally applied as a surface heat flow from the shoulder and a volumetric flow from the probe. Vinayak Malik et al [8] have used a CEL analysis model to study the effect of welding tool parameters in the plunge phase only applied on alloy AA2024-T3. Iordache Monica et al [9] have presented of a numerical model using the Arbitrary Lagrangian Eulerian (ALE) with adaptive remesh to simulate the plunge phase, the CPU time is 3 days and 16 hours for only the simulation time of 2.425 seconds. Some previous researches were provided pure thermal models without regard to the effect of mechanical stirring, while others built the model based on only one welding phase of the three phases of the process.

II. OBJECTIVES

The actual modling of the FSW process should include a thermo-mechanical coupling study during the three welding phases (plunge, dwell and traverse) at acceptable time. Hence, the importance of the research and its goal is to provide a comprehensive model that helps to choose the basic optimal parameters (rotation and traverse speeds) for the success of the actual welding process.

III. METHODOLOGY

1- The numerical modeling for a comprehensive FSW process was performed by Abaqus/ Explicit program based on a solid mechanical approach- CSM with mutual thermo- mechanical coupling using CEL analysis.

2- The implemented model was applied to obtain the optimal parameters of tool rotation speed and it's traverse, and the modeling results were verified experimentally by performing the welding process for an aluminum alloy using a vertical milling machine.

IV. NUMERICAL MODLING

The most important difficulties in building a numerical model are determining the appropriate modeling technique and choosing the best numerical approach to analysis. The techniques used in modeling are dependent on either CFD or CSM. CFD faces several challenges lead to a large modling error of welding temperature. CSM is only suitable for low strain rate plastic deformations. Since FSW is a process that includes thermo-mechanical coupling with high strain rates, this requires a large number of degrees of freedom, which consumes a long time and requires a large CPU. Therefore, choosing a suitable numerical approach for analysis in CSM technology determines the relationship between the mesh and the continuous deformation of the studied area and provides an accurate solution to the boundaries and interfaces, and it allows to modeling of plastic deformations with high strain rates in FSW [10,11], all of this needs a lot of accuracy and attention. The analysis approach varies to:

1- Lagrangian analysis: it cannot be adopted much in FSW because the extreme mesh distortion will lead to computation failure [12].

2- ALE and Adaptive remesh analysis: It maintains good mesh quality throughout the computation process except that it fails when the mesh distortion is very severe [13].

3- CEL Analysis: CEL analysis models have been developed to simulate severe plastic deformation processes such as rolling, cutting, friction extrusion and FSW. The CEL analysis shows a high computational efficiency for the extreme plastic deformation process without simulation failure, it combines the features of the Lagrangian and Eulerian mesh at the same time as shown in figure 2, where in Lagrangian nodes and elements are able to deform and move with deformation of the material, while in Eulerian both nodes and elements remain constant and only material can flow in the whole domain, it also has the advantage of not only solving deformation problems of the elements, but also accurately describes the physical limits of the material and reaches steady state in a relatively short time even with an acceptable mesh density to properly track the free surface [14,15,16].

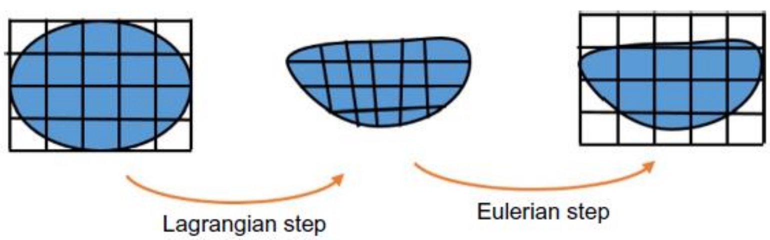

Figure. 2. Schematic of split operator for CEL method

Implementing a model for high deformations based on CEL analysis requires the use of a modeling program that has the ability to select a variety of elements, including those for CEL analysis, which are available in Abaqus program.

V. IMPLEMENTATION OF THE MODEL

The following paragraphs explain the stages of implementing the model:

1-Part: The probe was selected in a cylindrical shape with a diameter of 5 mm, a height of 4.5 mm, and the diameter of the shoulder was 16 mm. The plate is made of 6061-T6 aluminum alloy with dimensions (60×30 ×5) mm, figure 3. The tool was considered as 3D rigid part and the plate as the Eulerian part. The movement of the tool was controlled by a reference point to which the traverse and rotation are applied.

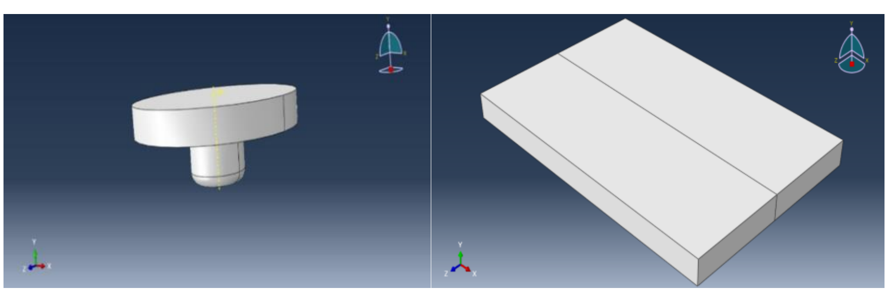

Figure. 3. Geometry of the parts of the welding process

2- Property: The plastic behavior of the plate was described using the Johnson- Cook law shown in equation 1:

$$\sigma y = [A + B(\bar{\varepsilon}^{pl})^n]\left[1 + c\left(\frac{\dot{\bar{\varepsilon}}^{pl}}{\dot{\varepsilon}_0}\right)\right]\left[1 - \left(\frac{T - T_{room}}{T_{melt} - T_{room}}\right)^m\right] \dots \dots (1)$$

where $\bar{\varepsilon}^{pl}$ is the effective plastic strain, $\dot{\bar{\varepsilon}}^{pl}$ is the effective plastic strain rate, $\dot{\varepsilon}_0$ is the normalizing strain rate and A: Yield stress, B: Strain factor, C: Strain rate factor, m: the exponent of temperature, n: the exponent of strain hardening effect, Troom: is the room temperature, Tmelt are material solidus temperature, T: Effective temperature[17]. The values of these constants are taken from Table 1 [18].and Table 2 shows the mechanical and thermal properties that change with temperature [19].

Table 1. Johnson-Coke material parameters for 6061-T6 alloy**.**

A	**B**	**C**	**m**	**n**	**Troom**	**Tmelt**
342	114	0.002	1.34	0.42	25	583

Table 2. Thermal and mechanical properties of 6061-T6 alloys**.**

Temperature ℃	**Density Kg/m3**	**elasticity's Modulus Pa**	**Poisson modulus**	**Specific heat J/kgC**	**Thermal expansion**
25	2690	6.69E+10	0.33	945	2.35E-05
100	2670	6.32E+10	0.334	978	2.47E-05
149	2670	6.13E+10	0.335	1000	2.57E-05
204	2660	5.63E+10	0.336	1030	2.66E-05
260	2660	5.12E+10	0.338	1052	2.76E-05
316	2630	4.72E+10	0.36	1080	2.85E-05
371	2630	4.35E+10	0.4	1100	2.96E-05
427	2600	2.88E+10	0.41	1130	3.07E-05
482	2600	2.02E+10	0.42	1276	**-**

It was considered that 90% of the plastic deformation is converted to heat which means that the inelastic working part is 0.9.

3- Step: The analysis was chosen of the type Dynamic Explicit Temperature- Displacement and the mass scaling feature was used.

4- Interaction: The contact between the tool and the Eulerian plate is of the general contact (Explicit) type in which the tangential behavior was described by the Coulomb Friction law with a coefficient of friction that varies with temperature as in the table 3 [20], and the normal behavior was described as Hard Contact and in Heat Generation it was considered that the entire frictional action turns into heat but about 30 % of this total heat is transferred to the tool.

Table 3. Temperature dependent friction coefficient of aluminum

Temperature ℃	**Friction Coefficient**
22.0	0.610
34.7	0.545
93.3	0.259
147.5	0.115
210.6	0.064
260.0	0.047
315.6	0.035
371.1	0.020
426.7	0.007
583.0	0

5- Load: At this stage, the boundary conditions were represented by fixing the plate and determining the rotation and traverse speeds of the reference point of the tool according to the three welding phases. The Amplitude in the Tabular pattern for displacement and the smooth step pattern for the speed of the traverse were used, also the initial temperatures of both the tool and the plate were set at 25℃, the Boltzmann constant 5.766 E-008 and absolute zero temperature -273.15.

6- Mesh: The element type EC3D8RT(8-node thermally coupled linear Eulerian brick, Hourglass control) was used for the Eulerian plate and with an element size equal 2, while the element type for the too C3D8RT(8-node thermally coupled brick, Trilinear displacement and temperature) with size equal 1.1, figure 4

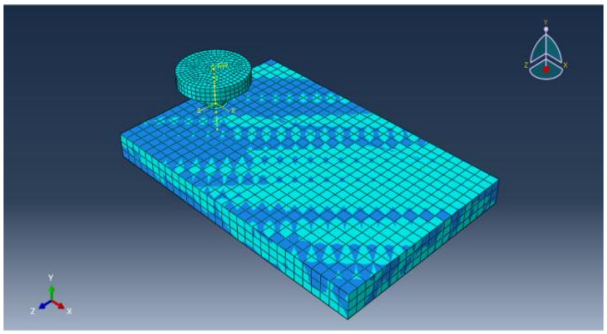

Figure. 4. The mesh in the model

The previous modeling steps were performed on six cases with different rotation and traverse speeds as shown in Table4. The solution model is 50 continuous hours for each case on: Intel (R) Core(TM) i5-8300H CPU@2.30GHZ, 64 bit, 16 Giga bit, Windows 10, Gaming Processor for all phases of welding process.

Table 4. Parametric study

case	Rotation speed	Traverse speed
1	630	60
2	630	150
3	1000	60
4	1000	150
5	315	60
6	315	150

VI. RESULT AND DISCUSSION

The following figures show the numerical results of Case No. 1 at the rotation speed 630 rpm and the traverse of 60 mm/min for the three phases of the welding process:

First, the plunge: this phase is considered as critical stage in modeling because most of the deformation that occurs here is result of contact and stirring action by rotation, which leads to the failure of the model, and this matter has been avoided by using CEL analysis. The heating occurs at this phase gradually and the temperature rises until it reaches the highest temperature in end of this phase (contact of the shoulder with the upper surface of the plate). Figure 5 shows the temperature at the end of the plunge phase of the plate, which reached 603.3 ℃, exceeding the melting point of 6061-T6 alloy.

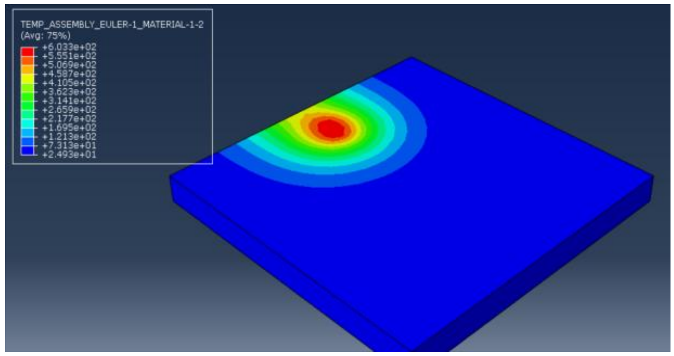

Figure.5. The temperature of the plung phase of the Eulerian plate

Second, the dwell: figure 6 shows the temperature distribution in the dwell phase, where the maximum temperature increased by a small amount to reach 605.5 ℃, and a larger distribution of the generated heat occurred. The temperature and its distribution here depend on the dwell time and the plunge speed of the tool and the temperature should not exceed the plasticity of the material.

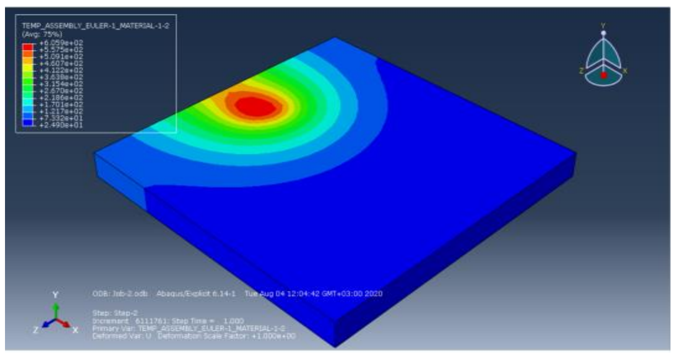

Figure.6. The temperature of the dwell stage of the Eulerian plate

Third, the welding: here the speed of traverse as such rotation speed contributes to controlling the amount of heat and stress generated. Figure7 shows the temperature distribution in the welding phase, figure8 shows the Nodal temperature diagram in the cross section of the joint at both sides of the weld seam.

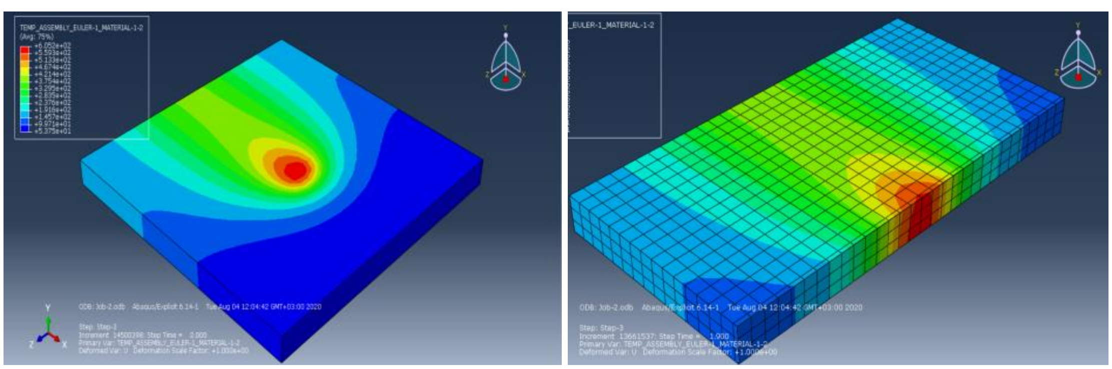

Figure.7. The temperature of the welding phase of the Eulerian plate

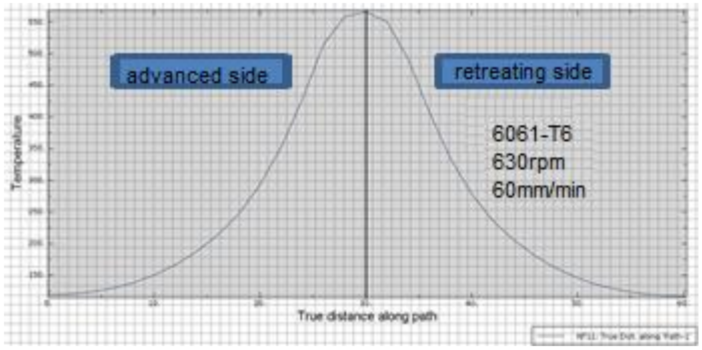

Figure.8. Nodal temperature diagram along the cross section of the weld.

Table 5 summarizes the maximum temperatures in each of the three welding phases for the six Cases.

Table 5. shows the maximum temperatures of the tool rotation and traverse speed studied for constant profile tool parameters

6061-T6	**Temperatures**		
Cases	**Plunge**	**Dwell**	**Traverse**
1	603.3	605.9	605
2	603.3	605.9	598.6
3	628.2	625.2	617.4
4	628.2	625.2	615.6
5	524.9	525.3	528.1
6	524.9	525.3	511.9

It is known that the final requirement for the FSW process is to create a certain amount of heat from friction heating and plastic deformation which keeps the material plate in good soft with an appropriate temperature. As we can see from table 5 that the rotational speed of the tool is the most controlling parameter of the frictional heat generation, as its effect on the thermal input appears from the beginning of the contact, causing an increase in interface temperature of the tool-plate in addition to the plastic deformation of the Eulerian plate due to stirring. In the welding phase, the speed of the traverse contributes to controlling the amount of heat generated with less effect. Table 5 also shows that when increasing the rotational speed while maintaining the traverse speed constant, the temperature reaches its maximum as a result of increasing the total thermal input at the interface of the tool-plate, and in contrast, we notice that the maximum temperature changes in the case of changing the traverse speed, where the temperature decreases with increasing the traverse speed at constant rotational speed.

The Graphic representation in figure 9 shows that the maximum temperature of the two rotation speeds (1000 and 630) rpm at the two traverse speed (60-150) mm/min give temperatures much greater than the melting point of the aluminum alloy.

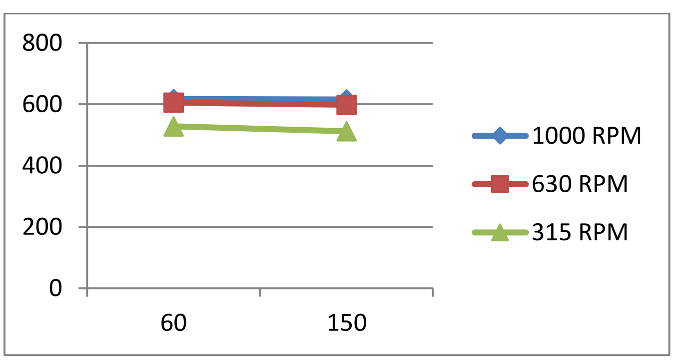

Figure. 9. Temperature chart at rotational speeds (315,630,1000) and traverse speed (60,150) of the plate

It was found that the rotational speed of 315 rpm is what achieves the required temperature value for the welding process of the studied alloy. As for the effect of the traverse speed, it is determined depending on the Von MISES stress during the welding phase, as shown in figure10 and the chart representation in Figure 11 where it was found that increasing in the traverse speed leads to higher stresses to which the plate was subjected.

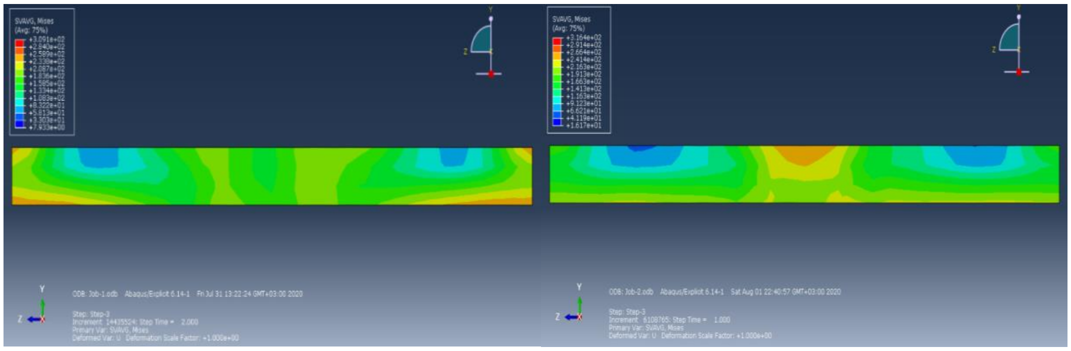

Figure. 10. SVAVG (Volume – averaged stress components at intergration points)Lift: 150mm/min, Right: 60mm/min at 315rpm

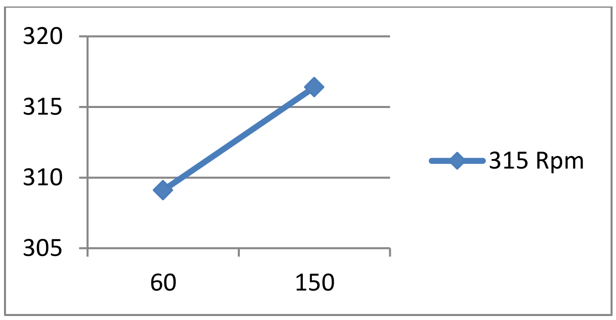

Figure.11. The stresses chart at 315 rpm, and (60, 150) mm/min during the welding phase.

The parametric study of the six cases has shown that the fifth case, in which the rotation speed of 315 rpm and the traverse is 60 mm /min, is the optimalcase for welding the aluminum plate 6061-T6, t should be mentioned that the heat loss in the convection of the environment and back plate, as well as the effect of the dimensions and profile of the tool, were not taken into consideration on heat generation.

Accordingly, this numerical results were verified by conducting an experimental test on a modified vertical milling machine to suit the friction stir welding machine, and the success of the welding process was demonstrated as in figures 12, 13.

Figure.12. experimental test for welding process with a rotating speed of 315rpm and a traverse speed of 60mm/ min

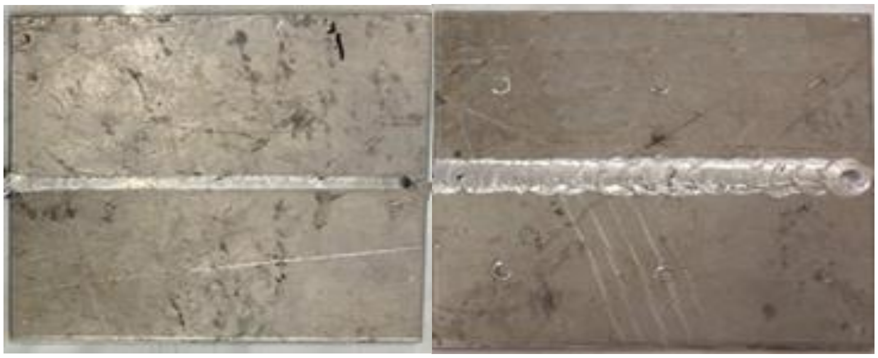

Figure.13. Welded aluminum plate with a rotational speed of 315rpm and a traverse of 60mm/ min

VI. CONCLUSIONS

In this paper, a non-linear, three-dimensional, coupled thermo-mechanical model was presented, that simulated The full phases of the FSW welding process (plunge, dwell and traverse), depending on a CEL analysis and using the Abaqus/ Explicit program. Also the model was used to clarify effect of changing both of the rotational speed (315, 630, 1000) rpm and the traverse speed (60, 150) mm/min in the maximum temperature and its distribution in addition to the stresses, applied to 6061-T6 aluminum alloy. The results lead to the following conclusions:

1- CEL analysis showed computational efficiency to model the extreme deformations that occur during the friction stir welding process through the parametric study of the models that were implemented.
2- The numerical results indicated that the temperature was approximately asymmetrically distributed during the three welding phases across the cross-section of the plate. In the plunge phase the temperature is gradually increased and in the dwell phase the heat is distributed across the plate while the temperature field became semi-stable in the welding phase.
3- The numerical modeling results of the parametric study were showed that the case where the rotation speed of 315 rpm and the traverse speed of 60 mm/min was the one that gave the appropriate temperature and stress for the welding process, among the other studied cases.
4- It was obtained a good agreement between numerical and experimental results.

REFERENCES

[1] P. Tanwar, V. Kumar, Friction Stir Welding: Review. *International Journal of Enhanced Research in Science Technology and Engineering, ISSN: 2319-7463 Vol. 3 Issue 10*, October-2014, pp: (172-176).

[2] A. Simar, Y. Bréchet, B. de Meester, A. Denquin, C. Gallais, T. Pardoen. Integrated modeling of friction stir welding of 6xxx series Al alloys: Process, microstructure and properties. *Progress in Materials Science*- 2012, 57.1: 95-183.

[3] O. Salih, H. Ou, W. Sun, D.G. McCartney, A Review of Friction Stir Welding of Aluminum Matrix Composites. Materials & Design, 86-2015,61-71.

[4] He, X., Gu, F., & Ball, A. A Review of Numerical Analysis of Friction Stir Welding. Progress in Materials Science, 65- 2014,1-66

[5] D. Mariano Neto, P. Neto, Numerical Modeling of Friction Stir Welding Process: A Literature Review M, *The International Journal of Advanced Manufacturing Technology*-2013, 65.1-4: 115-126.

[6] Muhsin J. J.1, Moneer H. Tolephih2 and Muhammed A. Effect of Friction Stir Welding Parameters (Rotation and Transverse) speed on the Transient Temperature Distribution in Friction Stir Welding of AA 7020-T53. *ARPN Journal of Engineering and Applied Sciences*- 2012, 7.4: 436-446.

[7] H. Li, D. Liu, Simplified Thermo-Mechanical Modeling of Friction Stir Welding with a Sequential FE Method. *International Journal of Modeling and Optimization*, 4(5)-2014, 410.

[8] V. Malik, Sanjeev, N. K, Hebbar, S. V Kailas. Investigations on The Effect of Various Tool Pin Profiles in Friction Stir Welding Using Finite Element Simulations. *Procedia Engineering, 97*-2014, 1060-1068.

[9] I. Monica, B. Claudiu, N. Eduard, I. Doina, *Numerical Simulation of Friction Stir Welding (FSW) Process Based on ABAQUS Environment*, In Solid State Phenomena Trans Tech Publications Ltd, Vol. 254-2016, (pp. 272-277).

[10] G. Chen, S. Zhang, Y. Zhu, C. Yang, Q. Shi, Thermo‑mechanical Analysis of Friction Stir Welding: A Review on Recent Advances, *Acta Metallurgica Sinica* (English Letters)-2020, 33.1: 3-12.

[11] B. Meyghani, M. B. Awang, S. Emamian, M. Khalid. M. Nor and S. Pedapati, A Comparison of Different Finite Element Methods in the Thermal Analysis of Friction Stir Welding (FSW), *Metals*- 2017, 7.10: 450.

[12] B. Meyghani; C. Wu, Progress in Thermomechanical Analysis of Friction Stir Welding. *Chinese Journal of Mechanical Engineering, Ji xie gong cheng xue bao*- 2020, 33.1.

[13] M.Ansari, A. Samanta, R. Behnagh, H. Ding, An Efficient Coupled Eulerian-Lagrangian Finite Element Model for Friction Stir Processing, *The International Journal of Advanced Manufacturing Technology*- 2019, 101.5-8: 1495-1508.

[14] RJain, S. K. Pal and S. B. Singh, Thermomechanical Simulation of Friction Stir Welding Process Using Lagrangian Method. *In Simulations for Design and Manufacturing*, Springer, Singapore-2018, (pp. 103-146)
[15] R. Jain, S. Pal, S. Singh, Numerical Modeling Methodologies for Friction Stir Welding Process, *Indian Institute of Technology, Kharagpur, India. Computational Methods and Production Engineering: Research and Development* -2017,125.
[16] M. Iordache, E. Niţu, C. Bădulescu, B. Radu, C. Ciuca, Finite Element Analysis of Thermal Distributions in Dissimilar Friction Stir Welding of Copper and Aluminum Alloy, *Sudarea Sincercarea Materlalor, Welding& Material Testing XXVIno.2*-2017.
[17] M. Nourani, A. S. Milani, S. Yannacopoulos, On The Effect Of Different Material Constitutive Equation in Modeling friction Stir Welding: A Review And Comparative Study on Aluminum 6061, International *Journal of Advances in Engineering & Technology*-2014, 7.1: 1.
[18] M. safari, J. Joudaki, Coupled Eulerian-Lagrangian (CEL) Modeling of Material Flow in Dissimilar Friction Stir Welding of Aluminum Alloys, *Iranian Journal of Materials Forming*, 6(2)-2019, 10-19.
[19] Z. Zhu, M. Wang, H. Zhang, X. Zhang, T. Yu and Z. Wu, A Finite Element Model to Simulate Defect Formation During Friction Stir Welding, Metals,7(7)- 2017, 256.
[20] M. AWANG, V. H. Mucino. Thermo-mechanical modeling of friction stir spot welding (FSSW) process: use of an explicit adaptive meshing scheme. *SAE Technical Paper*- 2005.